RSC Advances

ROYAL SOCIETY OF CHEMISTRY

www.rsc.org/advances

Photophysics of Tungsten-Benzylidyne complexes derived from *s*-indacene: Synthesis, Characterization and DFT Studies

Cesar A. Morales-Verdejo,*[a] Ximena Zarate,[a,b] Eduardo Schott,[a] Sebastián Correa,[a] Iván Martinez-Díaz.[a]

a).- Universidad Bernardo O Higgins, Departamento de Ciencias Químicas y Biológicas, Laboratorio de Bionanotecnología, General Gana 1780, Santiago, Chile.

b).- Dirección de Postgrado e Investigación, Universidad Autónoma de Chile, Av. Pedro de Valdivia 641, Santiago, Chile.

e-mail corresponding author: cesar.morales@ubo.cl

Abstract

The photophysics of the mono- and homobimetallic complexes of tungsten benzylidyne derived from *s*-indacene have been examined by using absorption and emission. Theoretical calculations of these compounds were carried out to gain further understanding of these novel molecular systems. Consistent with this prediction, each of the complexes displays a weak, mid-visible absorption band which is attributed to the d → π* transition. The tungsten complexes also exhibit luminescence with a lifetime in the 5-6 ns regime.

Keywords: Tungsten Benzylidyne; Homobimetallic complex; DFT.

1. Introduction

Transition metal-alkylidynes, also known as metal-carbyne complexes [1-4] have been extensively studied over nearly four decades since their discovery [5]. Much of the interest in these compounds has been focused upon their diverse and fascinating reactivity, specially the catalytic metathesis of alkynes [6-14]; although many other aspects of their chemistry have also been explored, including the luminescence properties of their electronic states where the excited-state electron-transfer reactions of transition metal chromophores are integral to homogeneous systems for artificial photosynthesis, dye-sensitized solar cells, and photoredox-based methods for organic synthesis, among other applications [15-27] and their utility as building blocks for electronic materials[28-36]. Regarding photophysical studies of the metal carbyne complexes of the half-sandwich type $Cp(CO)\{P(OMe)_3\}M{\equiv}C\text{-}R$, where M = Mo, W and R = Aryl, a reported was made by McElwee-White [37,38]. These complexes display weak absorption bands in the visible region and long-lived luminescence. Theoretical and spectroscopic studies indicate that the low energy band is associated with the HOMO → LUMO transition, which is dominated by the d(M) → π*(M≡C-Ar) configuration. The low intensity of the HOMO → LUMO transition indicates that it is a forbidden process; the transition is likely parity forbidden but spin-allowed (i.e. a singlet-singlet transition). The transition is parity forbidden due to significant degree of d-character in the HOMO and LUMO. The more intense near-UV band is associated with a spin-allowed π(M≡C-Ph) → π*(M≡C-Ph) transition, bearing some analogy to the π→π* transition of the Ph-C≡C-Ph chromophore. The emission lifetime of these complexes ranges from 50 to 250 ns, with quantum yields typically in the order of $5x10^{-4}$. The comparatively long excited state lifetimes coupled with relatively low radiative rate constant ($kr \approx 10^3\ s^{-1}$) strongly imply that the luminescent state has triplet spin character.

This contribution describes the general approach for the successful preparation of the mono- [$(CO)_2PhC{\equiv}W$(2,6-diethyl-4,8-dimethyl-5-hydro-*s*-indacenedide)] (**1**) and homobimetallic complexes [$\{(CO)_2PhC{\equiv}W\}_2$(2,6-diethyl-4,8-dimethyl-*s*-indaceneiide)] (**2**) in order to understand of the electronic properties allowing the intermetallic communication in this kind of systems. The *s*-indacene was chosen because this kind of ligands may connect two or more organometallic centers, which may have different oxidation states and allow interaction between them. The compounds derived from 1,5-dihydro-*s*-indacene, are obtained in high yields and are easy to manipulate, as well as selectively converting them into the corresponding mono- or dianions by means of a suitable strong base. In this context, these polyalkylated *s*-indacene compounds offer a unique opportunity for the synthesis of homo- and

heterobimetallic complexes by a stepwise insertion of different metallic fragments [55-58]. In addition, this kind of ligand of fused aromatic ring offers a planar backbone with a high delocalizability of their electron-rich π system, making it a perfect candidate for the redox fine-tuning. These molecular species was fully characterized by methods such as FT-IR, ^{1}H-NMR, and ^{13}C-NMR spectroscopic analysis as well as mass spectrometry. Theoretical calculations of these compounds were carried out to gain further understanding of these novel molecular systems.

2. Experimental Section

2.1 General Data

All manipulations were carried out under pure dinitrogen atmosphere using a Vacuum Atmospheres drybox equipped with a Model HE 493 Dri-Train purifier or a vacuum line using standard Schlenk-tube techniques. Reagent grade solvents were distilled under dinitrogen from sodium/benzophenone (tetrahydrofuran, toluene, petroleum ether) or from P_2O_5 (dichloromethane). The starting compounds [W≡CPh$(CO)_2(py)_2$Br], [39] and 2,6-diethyl-4,8-dimethyl-1,5-dihydro-s-indacene (Ic'H_2) [40] were prepared according to published methods. Elemental analyses (C and H) were made with a Fissions EA 1108 microanalyzer. ^{1}H and ^{13}C NMR spectra were recorded on Bruker AC-400, Bruker AC-200P and Bruker AC 80 Spectrometers. Chemical shifts were reported in ppm relative to residual solvents and were assigned using 2D NMR tools. All peaks reported were singlets, unless otherwise specified. Mass spectra (EI, 70 eV) were recorded on HP-5889A spectrometer. IR spectra on a Perkin-Elmer 1600 FT-IR spectrometer or Bruker Vector 22.

Electronic-absorption spectra were recorded using an Agilent Technologies 8453 UV-visible spectrophotometer of samples sealed in quartz cuvettes. Emission spectra were recorded on a PTI Quantmaster fluorimeter equipped with Peltier-cooled photomultiplier tube (R928) and InGaAs array detectors; emission intensities were corrected for instrument sensitivity.[41] Samples for absorption and emission measurements were prepared on vacuum line, degassed with multiple freeze/pump/thaw cycles, and sealed under purified nitrogen. Emission quantum yields were determined relative to [Ru$(bpy)_3$]Cl_2 in N_2-saturated H_2O (ϕem= 0.063),[42] using absorbance-matched reference and analyte samples; a correction for the refractive index of the solvent was applied.[43] Fluorescence lifetimes were measured with a ChronosBH time-domain fluorometer (ISS, Inc.) using timecorrelated single photon counting methods. The fluorometer contained Becker–Hickl SPC-130 detection electronics and an HPM-100-40 hybrid PMT

detector. Tunable picosecond pulsed excitation (lex=565 nm) was provided by a Fianium SC400 supercontinuum laser source and integrated acousto-optic tunable filter. Emission wavelengths were selected with bandpass filters (Semrock and Chroma). The instrument response function was measured to be approximately 120 ps FWHM, using a 1 % scattering solution of Ludox LS colloidal silica. Lifetimes were fit though a forward convolution method using the Vinci control and analysis software of the instrument; lifetimes were fit consistently within 5 %. The samples were photochemically stable for the duration of the lifetime measurements, as determined by electronic-absorption spectroscopy

2.2 Computational Details

All calculations were performed at density functional theory (DFT) level, as implemented in the Amsterdam density functional package (ADF2010).[44] The relativistic scalar and spin-orbit effects were incorporated via the Zeroth order regular approximation (ZORA) Hamiltonian.[45,46] Uncontracted type IV basis set were employed, using triple-ζ accuracy sets of Slater type orbitals (STO) with two polarization functions (TZ2P).[47,48] The ground and excited states were fully optimized via generalized-gradient approximation (GGA) employing the BP86 functional using UKS formalism.[49,50] The excitation energies were estimated by Time Dependent Density Functional Theory (TDDFT) using the LB94 model (Van Leeuwen and Baerends) which is specially designed for the calculation of optical properties and possesses a correct 1/r asymptotic behavior.[51-53] This methodology is based on the linear response formalism within the iterative Davison procedure implemented in the ADF2009 code. The calculations performed by first-principles method let to obtain accurate excitation energies. Solvent was included via COSMO model using THF as solvent.

2.3 Synthesis of [(CO)$_2$PhC≡W(η^5-2,6-diethyl-4,8-dimethyl-5-hydro-s-indacenide)], [(CO)$_2$PhC≡W(Ic'H)] **(1).**

A *n*-Butyllithium solution (1.6 M in hexanes, 0.52 ml, 0.80 mmol) was slowly added to a solution of 2,6.diethyl-4,8-dimethyl-1,5-dihydro-*s*-indacene (0.20 g, 0.80 mmol) in THF (30ml) at -80°C. The mixture was stirred for 2 h at room temperature to yield the monolithiated ligand. The solution was cooled to -80°C, and a solution of [W≡CPh(CO)$_2$(py)$_2$Br] (0.50 g, 0.90 mmol) in THF (30ml) was added via syringe. The mixture was allowed to reach room temperature and was then refluxed for 12 h. Then, the solvent was removed and the product was dissolved with diethyl ether, filtered to remove the insoluble LiBr, and washed three times. After removal of the solvent via vacuum, orange crystals were obtained. Yield: 90% (0.45 g).

Anal.Calc. for $C_{27}H_{26}O_2W$ (566.14 g·mol^{-1}): C: 57.26; H: 4.63. Found: C: 57.20; H: 4.61 %.

IR: (C≡O), 1978(s), 1887(s) cm^{-1}

^{1}H NMR (400 MHz, ppm in CD_2Cl_2): δ 0.80 (t, 6H, C*H*$_3$–CH$_2$–C$_{(2,6)}$); 2.34 (s, 6H, C*H*$_3$–C$_{(4,8)}$); 2.56 (q, 4H, CH$_3$–C*H*$_2$–C$_{(2,6)}$); 3.23 (s, 2H, C$_{(5)}$*H*); 4.67 (s, 2H, C$_{(1,3)}$*H*); 6.63 (s, 1H, C$_{(7)}$*H*); 7.37 (t, 2H, H$_m$-C$_6$H$_5$); 7.84 (t, 1H, H$_p$-C$_6$H$_5$); 9.14 (d, 2H, H$_o$-C$_6$H$_5$)

^{13}C NMR (100 MHz, ppm in CD_2Cl_2): δ 14.1 (*C*H$_3$-C$_{(4,8)}$); 14.7(C$_{(2)}$CH$_2$*C*H$_3$); 15.5(C$_{(6)}$CH$_2$*C*H$_3$); 25.3 (C$_{(6)}$*C*H$_2$CH$_3$); 30,5 (C$_{(2)}$*C*H$_2$CH$_3$); 40.2 (C$_{(1,3,5,7)}$); 122.5 (C$_{(7)}$); 124.4 (C$_{(2)}$); 125.9 (C$_{(6)}$); 128.6(C-C$_6$H$_5$); 129.9(C$_m$-C$_6$H$_5$); 129.6(C$_p$-C$_6$H$_5$); 138.9,141.2, 151.0, 154.3 (C$_{(3a,4,4a,7a,8,8a)ar\text{-}indacene}$); 154.4 (C$_o$-C$_6H_5$); 221.4 (CO); 259.9 (W≡C).

Mass spectroscopy results: MS (EI, m /z, %): [M]•+567; [M$^+$-((CO)$_3$PhC≡W))]•+ 236.

INSERT HERE CHART 1

2.4 Synthesis of [{(CO)$_2$PhC≡W}$_2$(η^5-2,6-diethyl-4,8-dimethyl-s-indacenediide)], [{(CO)$_2$PhC≡W}$_2$(Ic')] **(2).**

To a solution of 2,6-diethyl-4,8-dimethyl-1,5-dihydro-*s*-indacene (0.20 g, 0.80 mmol) in THF (30 ml) at -80°C, was added dropwisely a *n*-Butyllithium solution (1.6 M in hexanes, 1.06 ml, 1.7 mmol) with constant stirring. The mixture was stirred for 2 h at room temperature, producing the consequent lithiated salt of *s*-indacene ligand. Then the mixture was once again cooled at -80°C, and a solution of [W≡CPh(CO)$_2$(py)$_2$Br] (0.96 g, 1.70 mmol) in THF (30 ml) was added via syringe. The solution was allowed to warm to room temperature and was then refluxed for 12 h. Then, the solvent was removed and the product was extracted with hexanes filtering out the LiBr precipitate and washed five times with hexanes. After removal of the solvent via vacuum, red powder were obtained. Yield: 56 % (0.32 g).

Anal.Calc. for $C_{30}H_{30}O_4W_2$ (709.06 g·mol^{-1}): C: 48.35; H: 3.38. Found: C: 48.23; H: 3.19 %.

IR: (C≡O), 1979(s), 1890(s) cm^{-1}.

^{1}H NMR (400 MHz, ppm in CD_2Cl_2): δ 0.87 (t, 6H, C*H*$_3$–CH$_2$–C$_{(2,6)}$); 2.34 (s, 6H, C*H*$_3$–C$_{(4,8)}$); 2.53 (q, 4H, CH$_3$–C*H*$_2$–C$_{(2,6)}$); 4.38 (s, 2H, C$_{(1,3,5,7)}$*H*); 7.19 (t, 2H, H$_m$-C$_6$H$_5$); 7.84 (t, 1H, H$_p$-C$_6$H$_5$); 9.14 (d, 2H, H$_o$-C$_6$H$_5$)

^{13}C NMR (100 MHz, ppm in CD_2Cl_2): δ 13.2 (*C*H$_3$-C$_{(4,8)}$); 14.1(C$_{(6)}$CH$_2$*C*H$_3$); 14.9(C$_{(2)}$CH$_2$*C*H$_3$); 24.7 (C$_{(2,6)}$*C*H$_2$CH$_3$); 29.7 (C$_{(7,5)}$); 39.9 (C$_{(1,3)}$); 123.6 (C$_{(2,6)}$); 125.4(C-C$_6$H$_5$); 128.1(C$_m$-C$_6$H$_5$); 129.2 (Cp-C$_6$H$_5$); 138.1,140.3, 150.7 (C$_{(3a,4,4a,7a,8,8a)ar-indacene}$); 153.5 (C$_o$-C$_6H_5$); 220.6 (CO); 263.2 (W≡C).

Mass spectroscopy results: MS (EI, m /z, 6 %): [M]•+ 893; [M•+- ((CO)$_2$PhC≡W))]•+ 567.

INSERT HERE CHART 2

3. Results and discussion

3.1. Syntheses of the complexes

We have explored new synthetic routes for the preparation of the novel tungsten benzylidyne mono- and homobimetallic complexes incorporating the 2,6-diethyl-4,8-dimethyl-1,5-dihydro-*s*-indacene (Ic'H2) as a bridging ligand (scheme 1). From the addition of one equivalent of [W≡CPh(CO)$_2$(py)$_2$Br] to the monolithiated intermediate [Li][Ic'H] in THF solution at -78° results the formation of the monometallic orange compound [(CO)$_2$PhC≡W(Ic'H)] (**1**) (90% yield from Ic'H$_2$). The homobimetallic complex is obtained using the dianionic species of *s*-indacene, [Li]$_2$[Ic'], and two equivalent of [W≡CPh(CO)$_2$(py)$_2$Br] in THF at -78 °C led the formation of the one isomeric form of [{(CO)$_2$PhC≡W}$_2$(Ic')] (**2**) as shown by FT-IR and NMR spectroscopic analysis. This compound was isolated as red powder in reasonable yield of 56%. These complexes present a moderate solubility in solvents such as pentane, hexane and THF and high solubility in dichloromethane, benzene and toluene.

INSERT HERE SCHEME 1

3.2. NMR and FT-IR considerations

The NMR spectrum of **1** is consistent with the coordination of the tungsten to the five-membered ring of the *s*-indacenide ligand at 4.67 ppm (fig.1). ^{1}H and ^{13}C NMR spectra show that compound **2** is formed as a single isomer, namely the *anti*-configuration (see scheme 1.*II* and fig. 2). As mentioned by Ceccon et. al., the isomer ratio depends on a combination of several factors including steric hindrance, nature of the ancillary ligand, and symmetry of the indacene ligand. [54,55] In our case, a possible explanation for the formation of only one isomer, could lie in the nature of the $(CO)_2PhC{\equiv}W$- fragment which has a bulky fragment attached to *s*-indacene. This could hinder the entry on the same side of the second fragment and thus selectively yield the *anti*-isomer, explaining the formation of only one isomer as the final product, as is usually observed experimentally.[56-59] ^{13}C NMR spectra of monometallic and homobimetallic complexes were assigned using 2D NMR tools. These spectra present remarkable features, corresponding to the carbon atom of the carbonyl and alkylidyne groups. For the monometallic complex **1** and homometallic complex **2**, the value chemical shift of the carbonyl and alkylidyne groups appears at about 220 and 263 ppm respectively, these values are in agreement with the tungsten alkylidyne reported in literature [37,38,60]. The signal corresponding to the alkylidyne groups in the bond W≡CPh is very weak, is not possible to see the satellites, and cannot be calculated the constant due the very low concentration of the species.

INSERT HERE FIGURE 1

INSERT HERE FIGURE 2

The infrared spectra of compounds **1** and **2** show two intense carbonyl stretching bands at 1887 and 1978 cm-1, consistent with local C_{2v} symmetry for the $(CO)_2W$- unit.

3.3. Electronic Absorption Spectra and Luminescence Studies

The absorption spectra of the tungsten benzylidyne **1** and **2** were measured in toluene solution at room temperature (table 1). The absorption spectra of the mono- and homobimetallic complexes exhibit two primary UV/visible absorption features: strong band at approximately 330 nm and a weaker broad absorption at about 450 nm (fig 3). As discussed McElwee-White [37,38] et. al., the low energy band are clearly related to those assigned as $d \rightarrow \pi^*$ MLCT for the similar compounds. This transition contains substantially more $d \rightarrow d$ character than the description "MLCT"

implies. The more intense absorption at 330 nm is assigned to $\pi \rightarrow \pi^*$ transitions of the W≡C-Ph chromophore. Regarding luminescence studies at room temperature for the complexes **1** and **2**, the excitation of **1** and **2** at 450 nm in toluene gave a fairly strong emission centred at 643 nm. Rather surprisingly, both compounds show emission at the same wavelength (fig. 4).

Each emission showed a very broad band, with a Stokes shift of about 190 nm (52631cm^{-1}) measured from the 450 nm band. This might be due to stretching of the metal-carbon triple bond or, more likely, bending of the carbyne ligand in the excited state. Bocarsly [15] and McElwee-White [37] have reported a similar Stokes Shift of 180 to 220 nm for different derivatives of tungsten alkylidyne and associate the luminescence with the low-lying MLCT state. Further explanation will be given with the theoretical calculation, *vide infra*.

INSERT HERE TABLE 1

INSERT HERE FIGURE 3

INSERT HERE FIGURE 4

The emission excitation spectra for **1** and **2** show that there is an excitation feature coincident with the lowest absorption band, indicating that the emission originates with the chromophore and not an impurity (fig 5).

Luminescence lifetimes and quantum yields of the two complexes were also determined (table 2). The quantum yields for the complexes **1** and **2** lie in the ranges $\Phi \approx 2 \times 10^{-3}$. The emission time dependence of **1** and **2** were monitored in toluene at 650 nm and followed an exponential decay. A linearized least-squares analysis of the data gave a lifetime of 5.6 ns for **1** and 6.3 ns for **2** at room temperature. As mentioned by McElwee-White [37] and coworkers, the short lifetime of these complexes suggest that its emissive state possesses either competitive nonradiative pathways to the ground state or additional thermally accessible excited states with rapid decay pathways.

INSERT HERE TABLE 2

INSERT HERE FIGURE 5

3.7. DFT studies

Two different molecular configurations are possible, depending on the fact that both M moieties lie on the same side of the indacenide plane (*syn*) or on different sides (*anti*). The geometry optimization of both *syn* and *anti* configurations of the homobinuclear compounds has been performed before [61] considering that the metal atoms coordinate the C_5 rings, as usually observed experimentally. [55-58] For obvious sterical reasons, [53-58] the *anti* configuration was always found to be slightly more stable that the *syn* configuration, therefore we have developed the theoretical calculations for the *anti* configuration.

As shown in the table 3, the geometrical parameters for the ground states and excited states of **1** and **2**, there are only small changes observed between both states. However, the δ parameter suffers an interesting decrease in both excited state for one of the tungsten atoms, which is explained due to the decrease of electron density on the metal W in the excited state, therefore the hapticity tends to η^5 in order to compensate this lack. Furthermore, a large change is observed between the ground and the excited state in the dihedral angle of the *s*-indacene ring with the alkylidyne ligand. In the ground state, a dihedral angle near to a linear form is observed, whereas in the excited state a large dihedral angle of around 30° is observed for both structures. In case of compound **2** the mentioned changes are only observed over one of the tungsten atoms, while the second tungsten atom remains almost unaltered.

The calculated λ_{max} absorption of **1** and **2** show an intense peak at 426 and 403 nm, respectively (figure 6). Those calculated transitions are in good agreement with the experimental band (449 and 450 nm, respectively, see table S2 Supporting Information). In both cases the calculated transition is of metal to ligand charge transfer (MLCT) and goes from an orbital composed mainly by d orbitals of the tungsten atom to an orbital located over the metal, alkylidyne and -CO ligands, suggesting that the low energy absorption is due to a parity forbidden singlet-singlet transition as was discussed by McElwee-White [37,38] (table 4). This excited state relaxes its structure through a totally symmetric vibration rotating the tungsten metallic atom (only one in **2**). These excited states relax to the ground state via a luminescent decay located experimentally at 650 nm for **1** and **2**. For **1** the emission decay was calculated at 609 nm and for **2** at 643 nm, see figure 6. In both cases the calculated emission wavelength are in good agreement with the observed experimental results. Furthermore, the orbitals that are involved in the emission process, might give an explanation to the small change observed between **1** and **2**. As observed in **1**, the emission involves an excited state orbital located over the metal, alkylidyne and -CO ligand and the ground state orbital composed mainly by the *s*-indacene ligand. In **2** the emission involves an excited state orbital mainly located over

only one of the tungsten atoms and the ground state orbital with a similar composition to the same orbital in **1**. This observed behavior might give an explanation to the similarity observed between the emissions of both complexes.

INSERT HERE TABLE 3

INSERT HERE TABLE 4

INSERT HERE FIGURE 6

Conclusion

Low-valent carbyne complexes are well established compounds in organometallic chemistry, yet relatively few photophysical studies on these complexes have appear in the literature. In this work we have synthesized and fully characterized by means ^{1}H and ^{13}C NMR, and FT-IR spectroscopies, and mass spectrometry a novel mono- and homobimetallic tungsten benzylidyne complexes derived from *s*-indacene, $[(CO)_2PhC{\equiv}W\text{-}(Ic'H)]$ **1** and $[\{(CO)_2PhC{\equiv}W\}_2\text{-}(Ic')]$ **2**.

These complexes were examined in an effort to learn more about the excited states of these molecules, as well as to provide some information relevant to the study of photochemical reactions. DFT calculations and absorbance spectra indicate that possess low-lying excited states, which can be populated directly via parity-forbidden, singlet-singlet optical transition in the mid-visible region. For both complexes were observed the emission spectra which show short lifetime, suggesting its emissive state possesses either competitive nonradiative pathways to the ground state or additional thermally accessible excited states with rapid decay pathways.

Acknowledgements

The authors are grateful to Professor Juan Manuel Manriquez for his advice and discussion, Professor Michael D. Hopkins, Hunter B. Vibbert and Nathan La Porte from The University of Chicago for assistance with the photophysical experiments FONDECYT grants 11110273, 1130707 and 11140563 for the financial support.

References

1. M.A. Gallop, W.R. Roper, Adv. Organomet. Chem., **25** (1986) 121.

2. H.P. Kim, R.J. Angelici, Adv. Organomet. Chem., 27 (1987) 51.

3. A. Mayr, H. Hoffmeister, Adv. Organomet. Chem., 32 (1991) 227.

4. J.W. Herndon, Coord. Chem. Rev., 181 (1999) 177.

5. E.O. Fischer, G. Kreis, C.G. Kreiter, J. Müller, G. Huttner, H. Lorenz, Angew. Chem., Int. Ed. Engl., 12 (1973) 564.

6. R.R. Schrock, Acc. Chem. Res., 19 (1986) 342.

7. J.S. Murdzek, R.R. Schrock, IN Carbyne Comlexes; VCH Publishers: Weinheim, Gemany, 1988; pp 147.

8. X. Wu, C. G. Daniliuc, C. G. Hrib and M. Tamm,J. Organomet. Chem., 696 (2011) 4147.

9. R.R. Schrock, Chem. Commun., 49 (2013) 5529.

10. A. Fürstner, Angew. Chem., Int. Ed., 52 (2013) 2794.

11. B. Haberlag, X. Wu, K. Brandhorst, J. Grunenberg, C. G. Daniliuc, P. G. Jones and M. Tamm,Chem.–Eur. J., 16 (2010) 8868.

12. S. Beer, K. Brandhorst, C.G. Hrib, X. Wu, B. Haberlag, J. Grunenberg, P.G. Jones, M. Tamm, Organometallics, 28 (2009) 1534.

13. M.E. O'Reilly, I. Ghiviriga, K.A. Abboud, A.S. Veige, J. Am. Chem. Soc. 134 (2012) 11185.

14. M.E. O'Reilly, S.S. Nadif, I. Ghiviriga, K.A. Abboud, A.S. Veige, Organometallics 33 (2014) 836.

15. A.B. Bocarsly, R.E. Cameron, H.D. Rubin, G.A. MacDermott, C.R. Wolff, A. Mayr, Inorg. Chem. 24 (1985) 3976.

16. J. Carter, K.B. Kingsbury, A. Wilde, T.K. Schoch, C.J. Leep, E.K. Pham, L. McElwee-White, L. J. Am. Chem. Soc. 113 (1991) 2947.

17. S. Trammell, B.P Sullivan, L.M. Hodges, W.D. Harman, S.R. Smith, H.H. Throp, Inorg. Chem. 34 (1995) 2791.

18. T.K. Schoch, A.D. Main, R.D. Burton, L.A. Lucia, E.A. Robinson, K.S. Schanze, L. McElwee-White, Inorg. Chem. 35 (1996) 7769.

19. W.M. Xue, Y. Wang, T.C.W. Mak, CM. Che, J. Chem. Soc., Dalton Trans (1996) 2827.

20. W.M. Xue, M.C.W. Chan, T.C.W. Mak, C.M. Che, Inorg. Chem. 36 (1997) 6437.

21. F.W. Lee, M.C.W. Chan, K.K. Cheung, C.M. Che, J. Organomet. Chem. 563 (1998) 191.

22. F.W. Lee, M.C.W. Chan, K.K. Cheung, C.M. Che, J. Organomet. Chem. 552 (1998) 255. (

23. C.C.S. Cavalheiro, K.E. Torraca, K.S. Schanze, L. McElwee-White, Inorg. Chem. 38 (1999) 3254.

24. B.W. Cohen, B.M. Lovaasen, C.K. Simpson, S.D. Cummings, R.F. Dallinger, M.D. Hopkins, Inorg. Chem., 49 (2010) 5777.

25. B.M. Lavaase, J.. Locakard, B.W. Cohen, S. Yang, X. Zhang, C.K. Simpson, L.X. Chen, M.D. Hopkins. Inorg. Chem 51 (2012) 5660.

26. D.B. Moravec, M.D. Hopkins, Chem. Eur. J. 19 (2013) 17082.

27. D.B. Moravec, M.D. Hopkins, J. Phys. CHem. A 117 (2013) 1744.

28. J. Manna, S.J. Geib, M.D. Hopkins, J. Am. Chem. Soc. 114 (1992) 9199.

29. T.P. Pollagi, S.J. Geib, M.D. Hopkins, J. Am.Chem. Soc. 116 (1994) 6051.

30. H.A. Brison. T.P. Pollagi, T.C. Stoner, S.J. Geib, M.D. Hopkins, Chem. Commun. (1997) 1263.

31. M.P. Yu, A. Mayr, K.K. Cheung, J. Chem. Soc., Dalton Trans (1998) 475.

32. M.P.Y.Yu, K.K. Cheung, A. Mayr, J. Chem. Soc., Dalton Trans (1998) 2373.

33. A. Mayr, M.P.Y. Yu, V.W.W. Yam, J. Am. Chem. Soc. 121 (1999) 1760.

34. A. Mayr, M.P.Y. Yu, J. Organomet. Chem. 577 (1999) 577, 223.

35. K.D. John, M.D. Hopkins, Chem. Commun. (1999) 589.

36. D.C. O'Hanlon, B.W. Cohen, D.B. Moravec, R.F. Dallinger, M.D. Hopkins, J. Am. Chem. Soc. 136 (2014) 3127.

37. J.D. Carter, K.B. Kingsbury, A. Wilde, T.K. Schoch, C.J. Leep, E.K. Pham, L. McElwee-White J. Am. Chem. Soc., 113 (1991) 2947.

38. T.K. Schoch, A.D. Main, R.D. Burton, L.A. Lucia, E.A. Robinson, K.S. Schanze, L. McElwee-White Inorg. Chem., 35 (1996) 7769.

39. G.A., McDermott, A.M. Dorries, A. Mayr, Organometallics 6 (1987) 925.

40. M.R. Dahrouch, P. Jara, L. Mendez, Y Portilla, D. Abril, G. Alfonso, I Chávez, J.M. Manriquez, M. Riviere-Baudet, P. Riviere, A. Castel, J. Rouzaud, H. Gornitzka, Organometallics, 20 (2001) 5591.

41. Parker, C.A.; Rees, W.T. Analyst 85 (1960) 587.

42. Suzuki, K.; Kobayashi, A.; Kaneko, S.; Takehira, K.; Yoshihara, T.; Ishida, H.; Shiina, Y.; Oishic, S.; Tobita, S. Phys. Chem. Chem. Phys. 11 (2009) 9850.

43. J.V. Caspar, T.J. Meyer, J. Am. Chem. Soc. 105 (1983) 5583.

44. Amsterdam Density Functional (ADF) Code, Release 2010, Vrije Universiteit, Amsterdam, The Netherlands.

45. E. van Lenthe, E.J. Baerends, J.G. Snijders, J. Chem. Phys. 101 (1994) 9783.

46. G.T. Velde, F.M. Bickelhaupt, S. van Gisberger, C. Fonseca-Guerra, E.J. Baerends, J.G. Snijders, T. Ziegler, J. Comput. Chem. 22 (2001) 931.

47. J.G. Snijder, E.J. Baerends, P. Vernooijs, At. Data Nucl. Data Tables 26 (1982) 483.

48. Vernooijs, P.; Snijders, J.G.; Baerends, E.J. Slater Type Basis Functions for the Whole Periodic System, Internal Report, Free University of Amsterdam, The Netherlands, 1981.

49. A.D. Becke, Phys. Rev. A 38 (1988) 3098.

50. J.P. Perdew, Phys. Rev. B 33 (1986) 8822.

51. E. Runge, E.K.U. Gross, Phys. Rev. Lett. 52 (1984) 997.

52. F. Wang, T. Ziegler, E. van Lenthe, S. van Gisbergen, E.J. Baerends, J. Chem. Phys. 122 (2005) 204103.

53. R. van Leeuwen, E.J. Baerends, Phys. Rev. A 49 (1994) 2421.

54. S. Santi, A. Ceccon, A. Bisello, C. Durante, P. Ganis, L. Orian, F. Benetollo, L. Crociani, Organometallics 24 (2005) 4691.

55. A. Ceccon, A. Bisello, L. Crociani, A. Gambarro, P. Ganis, F. Manoli, S. Santi, A. Venzo, J. Organomet. Chem. 94 (2000) 600.

56. J.M. Manriquez, M.D. Ward, W.M. Reiff, J.C. Calabrese, N.L. Jones, P.J. Carroll, E.E. Bunel, J.S. Miller, J. Am. Chem. Soc., 117 (1995) 6182.

57. C. Adams, C. Morales-Verdejo, V. Morales, D. MacLeod-Carey, J.M. Manríquez, I. Chávez, A. Muñoz-Castro, F. Delpech, A. Castel, H. Gornitzka, M. Rivière-Baudet, P. Rivière, E. Molins, Eur. J. Inorg. Chem., (2009) 784.

58. D. MacLeod-Carey, C. Morales-Verdejo, A. Muñoz-Castro, F. Burgos, D. Abril, C. Adams, E. Molins, O. Cador, I. Chavez, J.M. Manriquez, R. Arratia-Perez, J.Y. Saillard, Polyhedron 29 (2010) 1137.

59. C. Morales-Verdejo, I. Martinez, D. Mac-Leod Carey, I. Chavez, J.M. Manríquez, D. Matioszek, N. Saffon, A. Castel, P. Rivière, E. Molins, Inorg. Chim. Acta, 394 (2013) 752.

60. S. Aderson, A.F. Hill, B.A. Nasir Organometallics 14 (1995) 2987.

61. M.T. Garland, S. Kahlal, D. Mac-Leod Carey, R. Arratia-Perez, J.M. Manrıquez, J.-Y. Saillard, New J. Chem., 35 (2011) 2136.

Tables

Table 1: Absorption Spectra of $[(CO)_2PhC{\equiv}W\text{-}(Ic`H)]$ and $[\{(CO)_2PhC{\equiv}W\}_2(Ic`)]$ in Toluene solution.

Complex	λ_{max}/nm	$\varepsilon_{max}/M^{-1}cm^{-1}$	Assignment
$[(CO)_2PhC{\equiv}W\text{-}(Ic`H)]$ (**1**)	330	7000	$\pi(W{\equiv}C\text{-}Ph) \rightarrow \pi^*(W{\equiv}C\text{-}Ph)$
	449	60	$d(W) \rightarrow \pi^*(W{\equiv}C\text{-}Ph(CO)_2)$
$[\{(CO)_2PhC{\equiv}W\}_2(Ic`)]$ (**2**)	330	7000	$\pi(W{\equiv}C\text{-}Ph) \rightarrow \pi^*(W{\equiv}C\text{-}Ph)$
	450	60	$d(W) \rightarrow \pi^*(W{\equiv}C\text{-}Ph(CO)_2)$

Table 2: Emission data.

Complex	λ (nm)	τ (ns)	Φ
$[(CO)_2PhC{\equiv}W\text{-}(Ic`H)]$ (**1**)	646	5.6	2.28×10^{-3}
$[\{(CO)_2PhC{\equiv}W\}_2(Ic`)]$ (**2**)	646	6.3	2.90×10^{-3}

Table 3: Selected bond distances (Å), angles and the calculated δ of the compounds **1** and **2**.

Parameter	Complex 1	Complex 1*S	Complex 2	Complex 2*S
d W1-C_2	2,351	2,454	2,335	2,433
d W1-$C_{1,3}$ [c]	2,368	2,387	2,361	2,374
d W1-$C_{3a,8a}$ [c]	2,549	2,441	2,589	2,427
d W2-C_6	-	-	2,336	2,333
d W2-$C_{5,7}$ [c]	-	-	2,362	2,388
d W2-$C_{4a,7a}$ [c]	-	-	2,583	2,606
dihedral W1-C	-3,0	-38,9	0,0	-30,6
dihedral W2-CBz	-	-	0,0	2,6
d W1-CO Average	1,981	1,975	1,987	1,989
d W2-CO Average	-	-	1,987	1,986
d W1-C	1,831	1,883	1,825	1,877
d W2-C	-	-	1,825	1,825
δW1	8	-1	11	0
δW2	-	-	11	12

$\delta = [(W\text{-}C_{3a,8a})-(W\text{-}C_2)]/W\text{-}C_2$

Table 4: Selected Orbital Energies and Compositions.

Compound	Transition	Orbital	% Composition	
1	$5\gamma_{1/2} \rightarrow 10\gamma_{1/2}$	$5\gamma_{1/2}$	W	39
			≡CPh	36
			CO	13
			Ic'H	12
		$10\gamma_{1/2}$	W	12
			≡CPh	59
			CO	20
			Ic'H	9
2	$4\gamma_{1/2} \rightarrow 10\gamma_{1/2}$	$4\gamma_{1/2}$	W	45
			≡CPh	3
			CO	26
			Ic'	26
		$10\gamma_{1/2}$	W	9
			≡CPh	32
			CO	45
			Ic'	14

Charts, Schemes and Figures

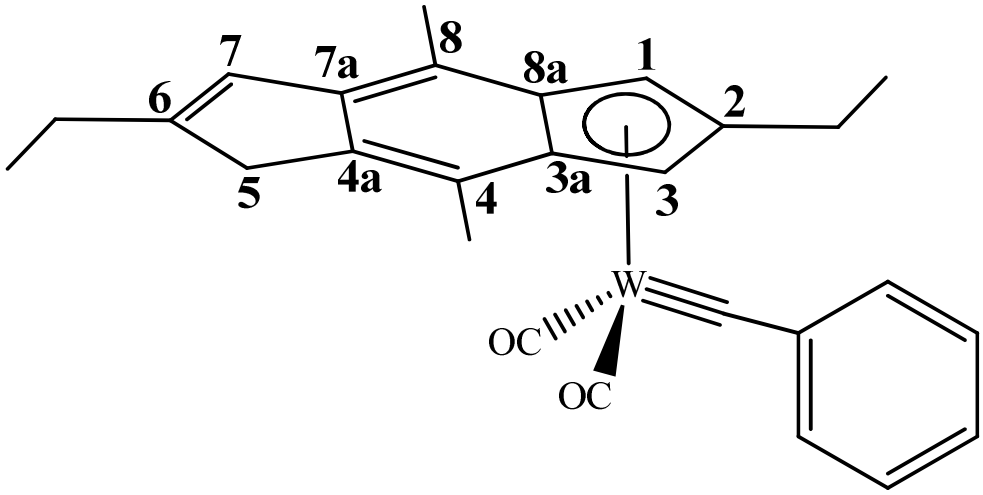

Chart 1. NMR assignment of the tetraalkylated *s*-indacene ligand for the here reported complex. [$(CO)_2$PhC≡W(Ic'H)] **1.**

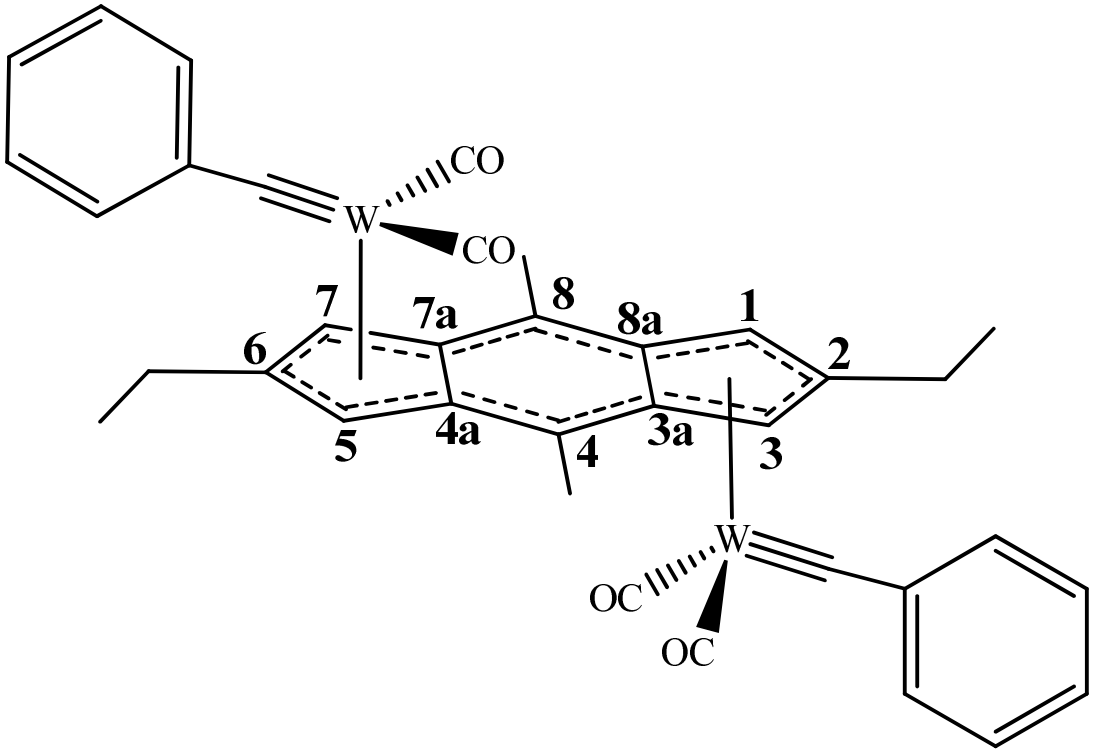

Chart 2. ^{1}H-NMR assignment of the tetraalkylated *s*-indacene ligand for the here reported complex. [{$(CO)_2PhC{\equiv}W\}_2$(Ic')] **2**.

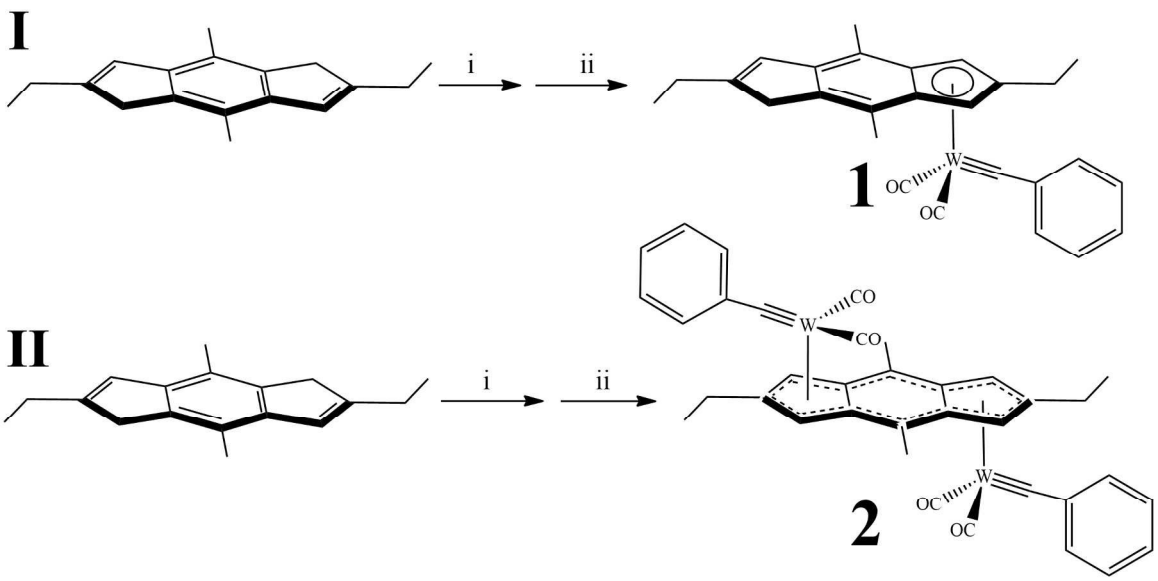

Scheme 1:
*Reagents **I***: **i**, *n*-BuLi (1 equiv), THF, -78° C (10 min), r.t. (1 h); **ii**, [W≡CPh(CO)$_2$(py)$_2$Br] (1 equiv), THF, -78° C, reflux. (12 h).
*Reagents **II***: **i**, *n*-BuLi (2 equiv), THF, -78° C (10 min), r.t. (1 h); **ii**, [W≡CPh(CO)$_2$(py)$_2$Br] (2 equiv), THF, -78° C, reflux (12 h).

Figures

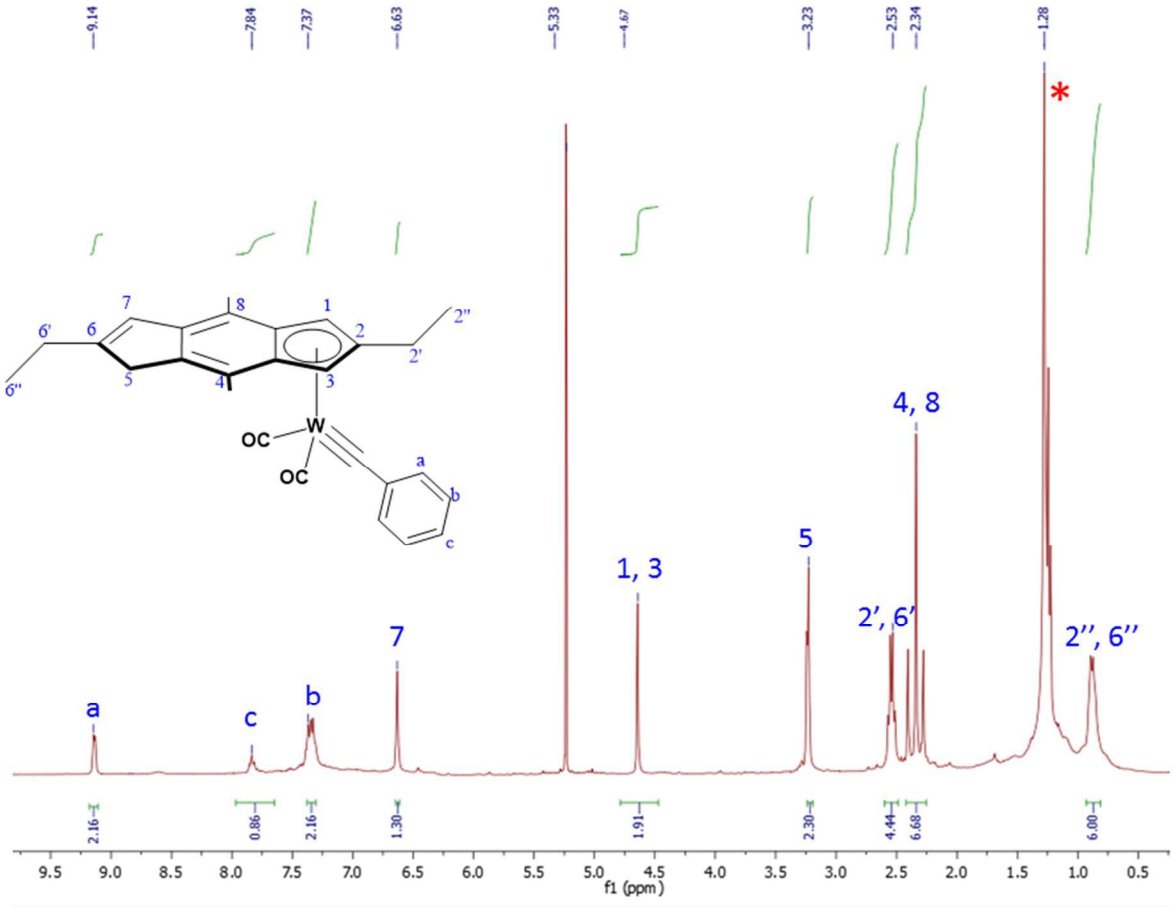

Figure 1: ^{1}H NMR spectrum of monometallic complex [$(CO)_2PhC{\equiv}W$-(η^5-2,6-diethyl-4,8-dimethyl-*s*-indacenide)] **1** in CD_2Cl_2.

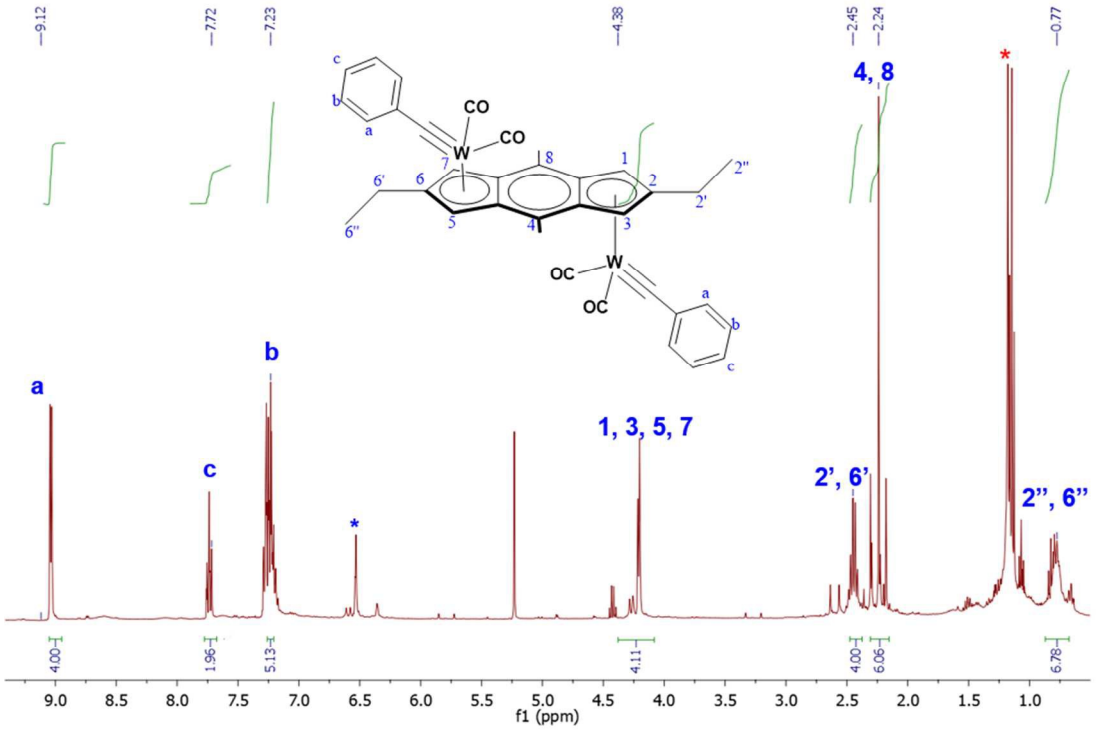

Figure 2: ^{1}H NMR spectrum of homobimetallic complex [{$(CO)_2PhC{\equiv}W\}_2$-(η^5-2,6-diethyl-4,8-dimethyl-*s*-indacenediide)] **2** in CD_2Cl_2. (* ligand free and grease)

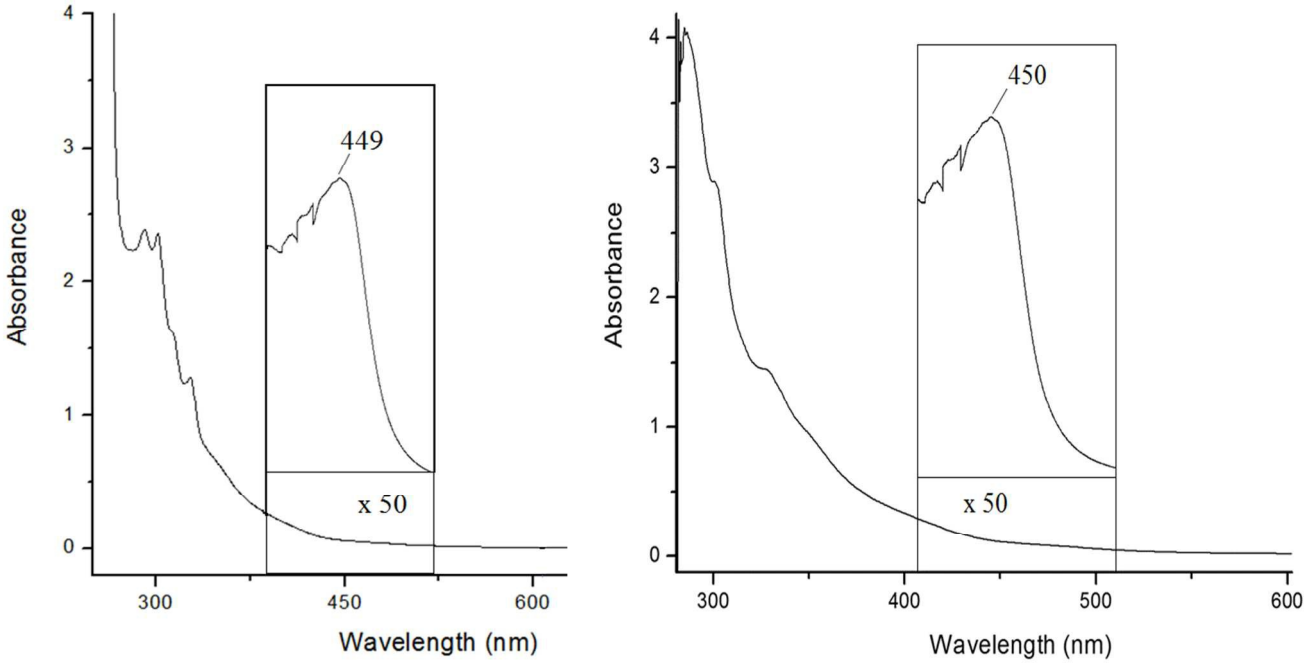

Figure 3. Absorption spectrum of the $[(CO)_2PhC{\equiv}W(Ic'H)]$ **1** and $[\{(CO)_2PhC{\equiv}W\}_2\text{-}(Ic')]$ **2** complexes. The solutions are $1x10^{-4}$ M in toluene at room temperature**.**

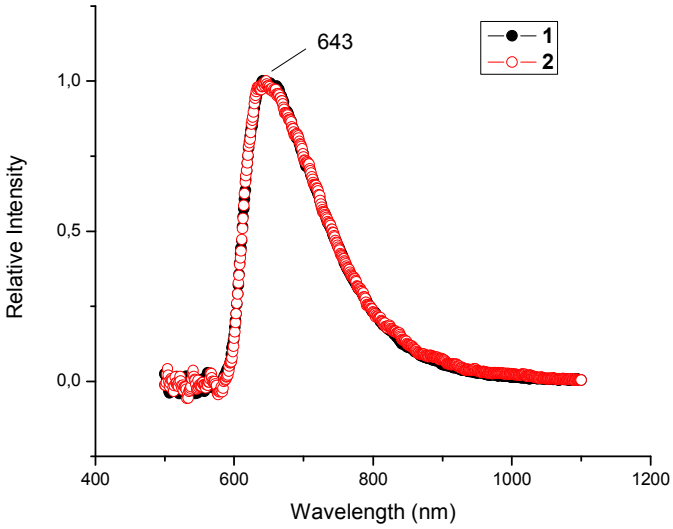

Figure 4. Emission spectrum of the [$(CO)_2$PhC≡W-(Ic'H)] **1** and [{$(CO)_2$PhC≡W}$_2$-(Ic')] **2** complexes. The solutions are 1x10^{-4} M in toluene at room temperature**.**

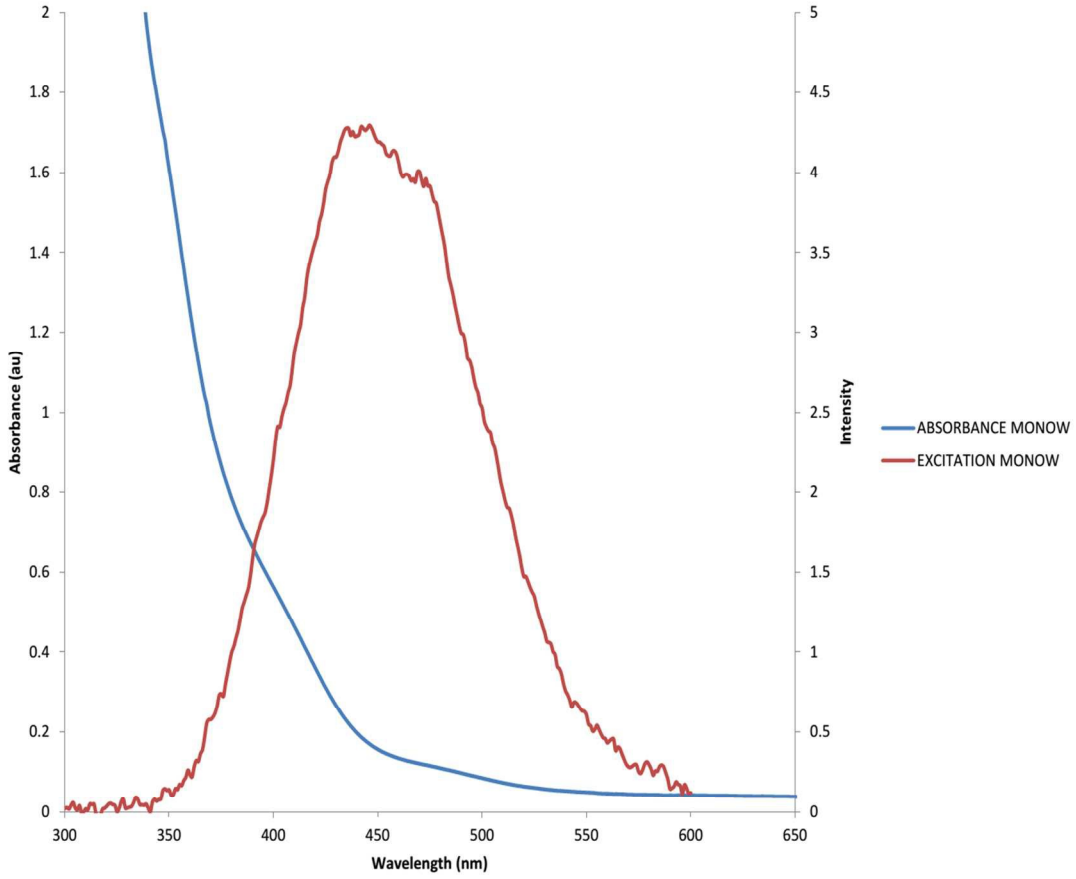

1

2

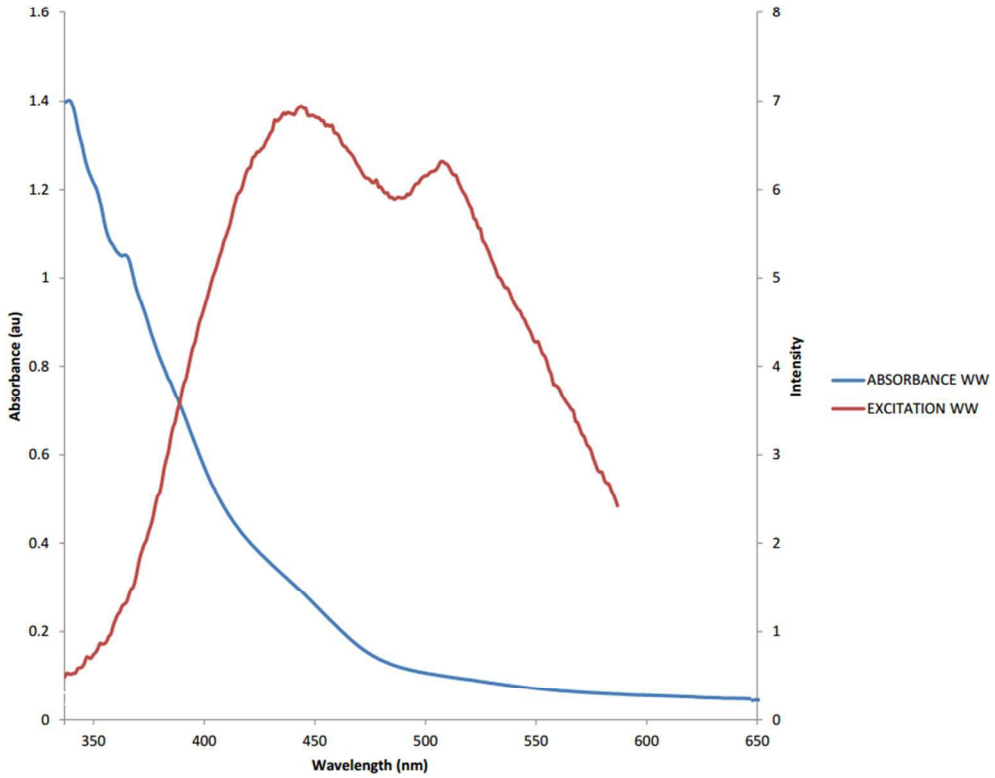

Figure 5. Emission Excitation Spectrum of the $[(CO)_2PhC{\equiv}W\text{-}(Ic'H)]$ **1** and $[\{(CO)_2PhC{\equiv}W\}_2\text{-}(Ic')]$ **2** complexes. The solutions are $1x10^{-4}$ M in toluene at room temperature**.**

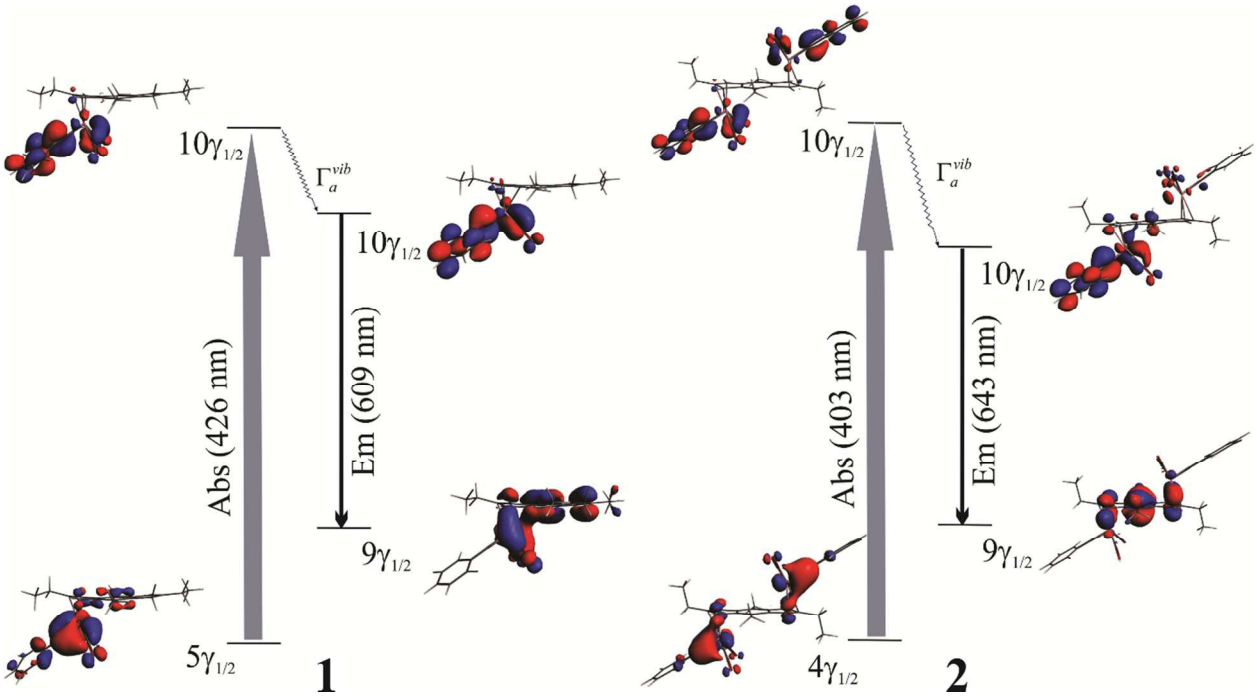

Figure 6. Diagram of the purposed luminescent process on synthesized compound $[(CO)_2PhC{\equiv}W\text{-}(Ic'H)]$ **1** and $[\{(CO)_2PhC{\equiv}W\}_2\text{-}(Ic')]$ **2**